STRESS-WAVE MEASUREMENTS ON LARGE RAYMOND-TYPE PILES

J. SANCHEZ DEL RIO. Dragados y Construcciones. Spain
A. BERNAL. Intecsa. Spain

1. Introduction

Dragados y Construcciones, S.A. manufactures and drives Raymond-type piles. They are made in pieces 5 meters long; then they ar joined together and prestressed. They are 0,91 m (36") to 1,68 m (66") in diameter. They usualy have concrete strengh greater than 45 MN/m^2 (450 kg/cm^2) and net prestressing stress of 7,5-10 MN/m^2 (75-100 kg/cm^2).

Driving control was systematically done by means of driving curves: number of blows-driving resistance, computed with a computer code based on the Smith method.

To improve the driving control, Dragados y Construcciones, S.A. has got a P.D.A. analyzer of Pile Dynamics Corp. and the corresponding unit MINC-23, with its software, including the CAPWAP code.

The first results of the driving control with P.D.A. and CAPWAP are shown in this paper.

2. General description of the work and the ground

This stress-wave measurement control of Dragados y Construcciones was used firstly in the Gibraltar Intercar sea coal terminal wich is being built in Algeciras Bay.

The coal terminal consist on:

a) Connecting dock, perpendicular to the shore line, 208 m long. Water depth is 8 m to 32 m. It has 72 Raymond-type piles, 1,37 m (54") diameter, 15,24 cm (6") wall thickness, 35 to 55 m long.

b) Unloading dock, paralel to the shore line, for ships up to 240.000 T.D.W., 360 m long. Water depth is 23 to 32 m. It has 180 Raymond-type piles, 1,68 m (66") diameter, 15,24 cm (6") wall thickness, 45 to 55 m long. The vertical loads on these piles are 4-5 MN (400-500 Mp).

The subsoil is formed by a thick stratum of sandy and silty soil, lying on a substratum of dense sand and gravel. The figure nº 1 shows a schematic profil.

Several layers can be distinguished. They are described in the next paragraphs, indicating the average depths of change of strata under the unloading dock.

A. Superficially, with a thickness of 3,0 m, there is mud.

B. From 3,0 m to 21,0 m there is silty sand, SM, with 22% (average value) and 40% (maximum value) of fines, usually non plastic. Type C silt and clay lenses can be found in this layer. The average number of blows in the S.P.T. is N ≐ 32, and the average N value that could affect a given pile is N = 16. The sand grains are mainly siliceous and the average friction angle in CU triaxial tests is ϕ' = 33º.

C. From 21,0 m to 28,0 m there are silt and clay with 0-65% of sand (average 20%). They have low to medium plasticity and some organic material. The number of blows in the S.P.T. is 7 to 50, with an average value of N = 29, and the average N value that could affect a given pile is N = 7. the average friction angle in CU triaxial tests is ϕ' = 26º. The averaga compresibility coefficient in the oedometer is C_c = 0,230.

D. From 28,0 m to 42,0 m there are alternating layers of silty sand (type B) and silt and clay (type C).

E. Under 42,0 m, elevation -65 m to -70 m, there are dense sand and gravel.

The dock was designed as a piled structure, with friction piles, driven 15-20 m in the ground. The silt and clay C layer, a few meters under the point of the piles, is an important obstacle to this solution. Then, it was more neccesary to perform a good control of the piling operations.

The control program includes: (a) several vertical load and uplift tests on a 0,91 m (36") diameter Raymond-type pile; (b) driving control with the P.D.A. of the test pile and the 5-10% of the dock piles; and (c) CAPWAP analysis of the more interesting piles controlled with the P.D.A. Test pile and some other dock piles will be controlled in driving and in redriving.

3. Wave speed measurements

The measurement of the speed of the wave caused by striking with a hammer the end of a pile lying on the ground resulted extremaly difficult. The figure nº 2 shows a test with satisfactory result. The wave speed values obtained in this kind of test were:

C = 4,3 - 4,4 m/ms

The wave speed was also measured in the begining of the driving of P.D.A. controlled piles. The pile perfomance is near a free pile with several equidistant peaks in the velocity curve; see figure nº 3. The wave speed values obtained were generally in the range of:

C = 4,4 - 4,5 m/ms

All along the driving the interval 2L/c was observed. The differences between the raise to raise interval and the peak-to-peak interval were small and the wave spped values were variable, also in the driving of one given pile, in the range of:

C = 4,2 - 4,6 m/ms

In the foce or velocity curves the pile seems to be continious; the joints between sections have not visible influence.

4. Summary of results from the P.D.A.

Up to this moment load tests piles and connecting dock piles were driven and controlled. There are not yet the results of measurements on unloading dock piles.

Load tests piles and connecting dock piles were driven with a hammer Vulcan 0-40 (Weigh 177,8 KN, nominal large stroke 0,91 m, nominal short stroke 0,46 m). Pile diameter is 1,37 m (54"), except for the pile number 1 (the one tested), that is 0,91 m (36"). Pile length is 50 m except the S-15 (35 m) and the P-29 (55 m). Water depth is 20-25 m except in pile S-15 that is 11 m. Driven length varies from 18 m to 22,5 m.

The figure nº 4 shows the values of (a) transferred energy, (b) maximum computed tension, (c) force at impact and (d) static resistance (J_c = 0,12), obtained from the analyzer. In the last drawing there are also the point and total ultimate loads considered in the design from static computations.

The maximum transferred energy was 89 m.KN (54% of the nominal energy of the hammer). The pile 3R had a maximum tension of 5 MN (500 Mp) equivalent to 10 MN/m^2 (100 kg/cm^2) and became broken. The maximum static resistance was found in the piles in which the transfered energy was higher. It takes the values:

Pile	E,m.KN(m.Mp)	FMAX,MN(Mp)	CTEN,MN(Mp)	RSTC,MN(Mp)(Jc=0,12)
2	-	10,2 (1.020)	-	7,5 (750)
3R	89 (8,9)	12,2 (1.220)	5,0 (500)	6,5 (650)
3'	75 (7,5)	11,2 (1.120)	1,5 (150)	8,1 (810)
S-15	86 (8,6)	11,0 (1.100)	2,7 (270)	6,9 (690)

The static resistance is smaller in pile 3R, in wich tensión was higher. In the other piles, the static resistance during driving is about 75% of the corresponding ultimate loads considered in the design.

5. Load tests

A steel structure was built to perform the load tests. It is anchored on four piles 1,37 m (54") in diameter and 50 m length, that make a square with sides of 6,36 m. The pile tested has 0,91 m (36") in diameter and it is in the square's center.

The tests had the following sequence:

a) Driving of all the five piles. The central one up to 16,30 m in depth, with a hammer Vulcan 0-40 in short stroke.

b) Compression vertical test up to 3,5 MN (350 Mp).

c) Uplift test up to 2,2 MN (220 Mp).

d) Redriving of the test pile up to 18,40 m in depth with a hammer Vulcan 0-30 in large stroke.

e) Compression vertical test up to 5,0 MN (500 Mp).

f) Uplift test up to failure, reached at 2,6 MN (260 Mp).

The central pile was instrumented with fourteen vibrating wire strain gauges, distributed in seven levels in two diametrically opposed lines.

Shaft and point load distribution was measured, as shown in the figure nº 5 for the 5,0 MN (500 Mp) compression vertical test. The maximum shaft transferred load was 2,7 MN (270 Mp), similar value to the ultimate uplift load, 2,6 MN (260 Mp).

The figure nº 6 shows the top load-settlement relationship in the 5 MN (500 Mp) compression test. It can be seen that failure is not reached.

6. Capwap analysis

The end of driving and the blows of maximun resistance in redriving of the central, 0,91 m in diameter, pile has been analyzed with CAPWAP.

The figures nº 7 and 8 show forces and velocities measured, and the figures nº 9 and 10 show the curves adjusted with CAPWAP.

The pile model was in both cases:

Total length	50,0 m
Length under gages	48,25 m
Driven length	16,5 m
Area of pile	3.140 cm^2
Wave speed	4,6 m/ms
Elastic modulus	5,4 KN/m^2 (540 Mp/cm^2)

In the restriking analysis, one section, five meters in length (from 20 m to 25 m over the point) with wave speed of 5,0 m/ms was considered in order to get a better adjustment between both force and velocity curves in that section.

The principal results of CAPWAP analysis were:

	End of driving	Redriving
Quake, cm, shaft/toe	0,3/0,3	0,22/0,2
Case damping (Jc), shaft/toe	0,2/0,2	0,35/0,35
Shaft resistance, MN (Mp)	0,9(90)	3,85(385)
Point resistance, MN (Mp)	2,6(260)	2,15(215)
Static resistance, MN (Mp)	3,5(350)	6,0(600)
Resistance ratio	1,00	1,71

For the same blows the P.D.A. gave:

	End of driving	Redriving
Transfered energy, m.KN (m.Mp)	35(3,5)	52(5,2)
Maximum force, MN (Mp)	6,2(620)	6,7(670)
Total resistance, MN (Mp)	5,4(540)	7,4(740)
Resistance ratio	1,00	1,37
Jc for RSTC = R_s, CAPWAP	0,27	0,23

The ultimate loads of the design from static computations in MN (Mp) were:

Driven length	Shaft Resist	Point Resist	Ultimate Resist
16 m	1,3(126)	3,1(313)	4,4(439)
18 m	1,6(161)	3,6(354)	5,2(515)

As it can be seen, the effect of restriking is very important. The end of driving P.D.A. or Capwap resistance underestimates the actual resistance. The restriking prediction is more accurate. The Case damping for this piles and this soils to be used in the analyser is near 0,2.

7. Conclusions

The driving control of Raymond-type piles with a P.D.A. and the analysis with CAPWAP has been implemented by Dragados y Construcciones, S.A., with promising results. It has help to improve the knowledge about the hammer and the pile, and to establish correlations between the desing resistance (computed with static formulas), the resistance obtained from the blown count (with the Smith's Wave equation), and the P.D.A. and CAPWAP static resistance in driving or redriving.

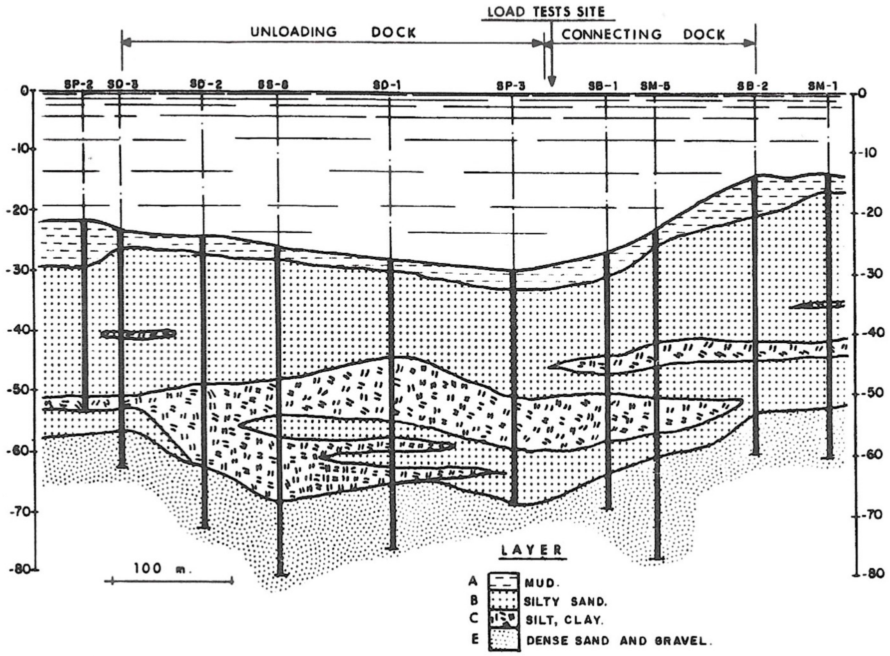

Fig. 1. Schematic ground profile under the coal terminal in Algeciras Bay.

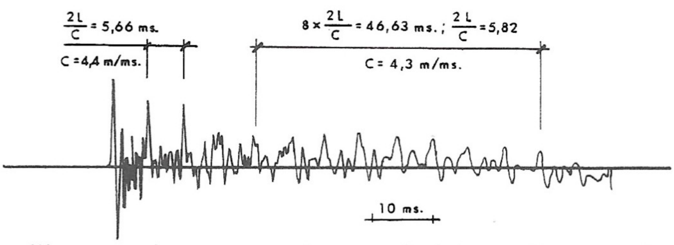

Fig. 2. Wave speed measurements on a pile lying on the ground.

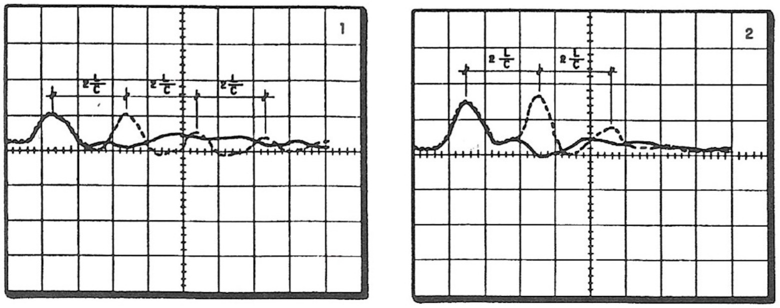

Fig. 3. Wave speed measurement at the begining of the driving.

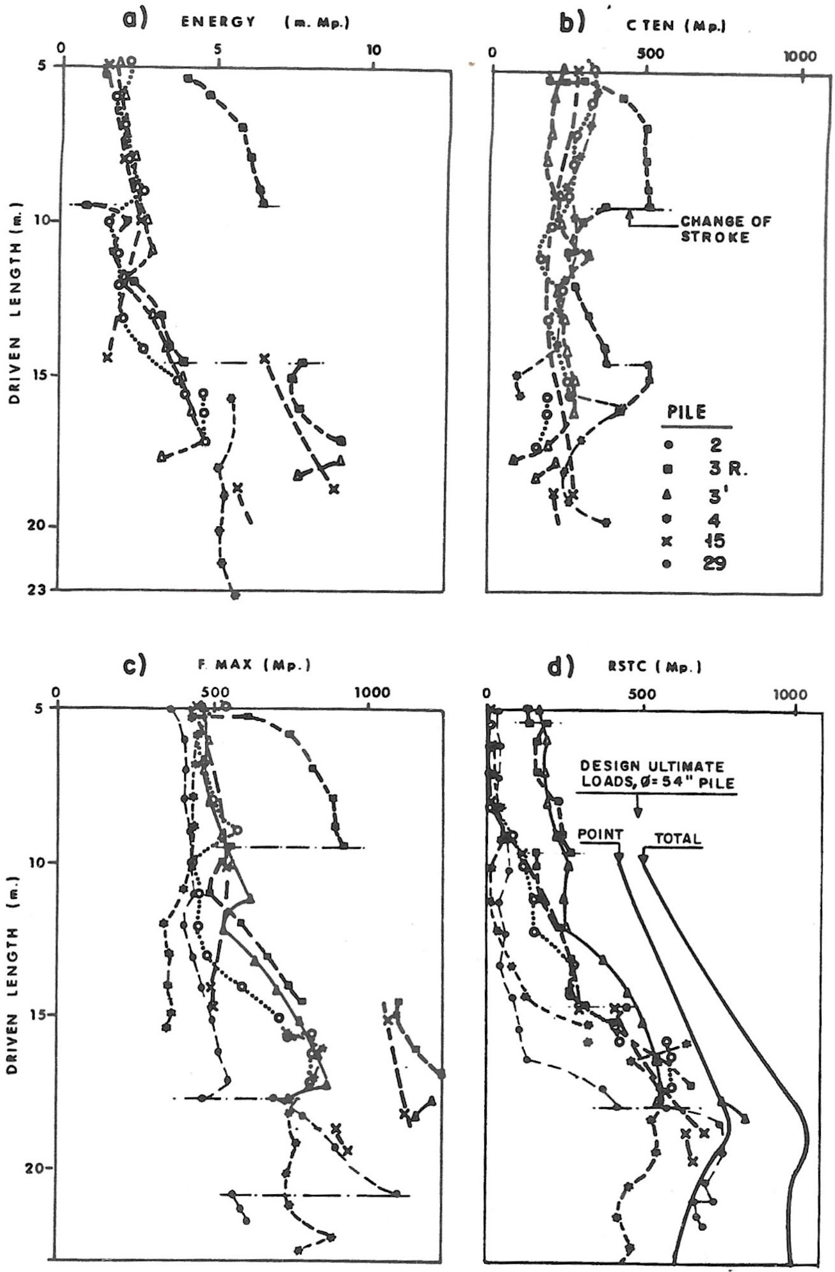

Fig. 4. P.D.A. results on Ø 54" piles.

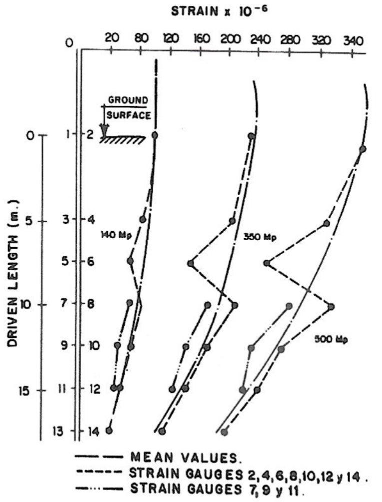

Fig. 5. Shaft and point load distribution in the compression vertical test.

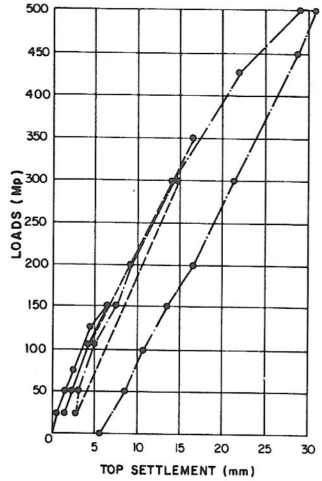

Fig. 6. Top load-settlement relationship in the compression vertical test.

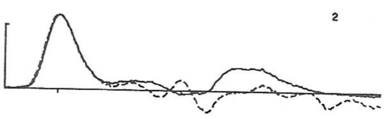

Fig. 7. PDA force and velocity curves. End of driving.

Fig. 8. PDA force and velocity curves. Redriving.

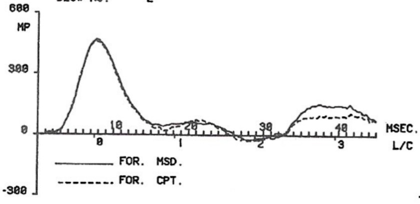

Fig. 9. CAPWAP analysis. End of driving.

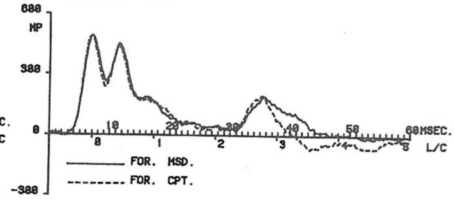

Fig. 10. CAPWAP analysis. Redriving.